AMERICAN SOCIETY of
GENE & CELL
THERAPY

A DNA Aptamer Targeting Galectin-1 as a Novel Immunotherapeutic Strategy for Lung Cancer

Yao-Tsung Tsai,[1] Chen-Hsien Liang,[1,2] Jin-Hsuan Yu,[3] Kuan-Chih Huang,[3] Chia-Hao Tung,[1] Jia-En Wu,[1] Yi-Ying Wu,[4,5] Chih-Hsien Chang,[2] Tse-Ming Hong,[1,4,5] and Yuh-Ling Chen[1,3]

[1]Institute of Basic Medical Sciences, College of Medicine, National Cheng Kung University, Tainan, Taiwan; [2]Institute of Nuclear Energy Research, Taoyuan, Taiwan; [3]Institute of Oral Medicine, College of Medicine, National Cheng Kung University, Tainan, Taiwan; [4]Institute of Clinical Medicine, College of Medicine, National Cheng Kung University, Tainan, Taiwan; [5]Clinical Medicine Research Center, College of Medicine, National Cheng Kung University, Tainan, Taiwan

Galectin-1 (Gal-1) is a pleiotropic homodimeric β-galactoside-binding protein with a single carbohydrate recognition domain. It has been implicated in several biological processes that are important during tumor progression. Several lines of evidence have indicated that Gal-1 is involved in cancer immune escape and induces T cell apoptosis. These observations all emphasized Gal-1 as a novel target for cancer immunotherapy. Here, we developed a novel Gal-1-targeting DNA aptamer (AP-74 M-545) and demonstrated its antitumor effect by restoring immune function. AP-74 M-545 binds to Gal-1 with high affinity. AP-74 M-545 targets tumors in murine tumor models but suppresses tumor growth only in immunocompetent C57BL/6 mice, not in immunocompromised non-obese diabetic (NOD)/severe combined immunodeficiency (SCID) mice. Immunohistochemistry revealed increased CD4+ and CD8+ T cells in AP-74 M-545-treated tumor tissues. AP-74 M-545 suppresses T cell apoptosis by blocking the binding of Gal-1 to CD45, the main receptor and apoptosis mediator of Gal-1 on T cells. Collectively, our data suggest that the Gal-1 aptamer suppresses tumor growth by blocking the interaction between Gal-1 and CD45 to rescue T cells from apoptosis and restores T cell-mediated immunity. These results indicate that AP-74 M-545 may be a potential strategy for cancer immunotherapy.

INTRODUCTION

Cancer immune escape plays a critical role in cancer progression. Tumor cells evolve multiple mechanisms to evade immune recognition or to regulate immune cell functions. Therefore, some therapeutic strategies have been developed to block the inhibitory signals received by T cells through cytotoxic T lymphocyte-associated antigen 4 (CTLA-4) or programmed cell death-1 (PD-1).[1,2] However, not all cancer patients respond to these immunotherapies, suggesting additional immunoregulatory mechanisms.[3,4] Thus, more strategies designed to control cancer immune escape are very important.

Galectin-1 (Gal-1) is a member of the galectin family of β-galactoside-binding proteins.[5] Previous studies have indicated that Gal-1 is highly expressed in many kinds of tumors and in the tumor stroma.[6–8] Since 1995, Gal-1 has been found to induce the apoptosis of T cells. Gal-1

triggers T cell apoptosis by redistributing and segregating the clustering of CD3 and CD45 and the clustering of CD7 and CD43 into membrane microdomains.[9] Gal-1 also acts as an antagonist in T cell receptor (TCR) signal transduction.[10] Furthermore, a previous study on head and neck cancer revealed a strong inverse correlation between Gal-1 and CD3 expression.[11] The first *in vivo* evidence of Gal-1-mediated immune regulation and tumor immune escape was demonstrated in a study on melanoma.[12] Gal-1 knockdown in melanoma cells slowed tumor growth by decreasing T cells apoptosis. In lung cancer, cancer-derived Gal-1 activated lung cancer-associated fibroblasts and triggered the tryptophan 2,3-dioxygenase (TDO2)/kynurenine axis, which impaired T cell differentiation and function.[13] In addition to tumors, high Gal-1 expression in the tumor stroma also plays a role in immunosuppression. Gal-1 is highly expressed in activated pancreatic stellate cells and induces T cell apoptosis in pancreatic cancers.[14] Stromal Gal-1 can maintain the immunosuppressive microenvironment in pancreatic cancer. Taken together, these results show that Gal-1 acts as an immune suppressor by directly promoting T cell apoptosis or indirectly impairing T cell differentiation in tumor cells and their microenvironment. Therefore, Gal-1 could be a potential therapeutic target in cancer immunotherapy.

Aptamers are one of the new technologies applied to pharmacy and diagnosis. Aptamers are single-stranded DNA (ssDNA) or RNA molecules that bind to specific target molecules with high affinity and specificity. Similar to antibodies, some aptamers can antagonize the activity of target proteins such as VEGF[15] and TLR2.[16] For example, the TLR2 aptamer has been reported to inhibit the TLR2-mediated immune response by blocking the activities of the TLR2 and TLR2 downstream pathways.[16] In addition to functional aptamers, some
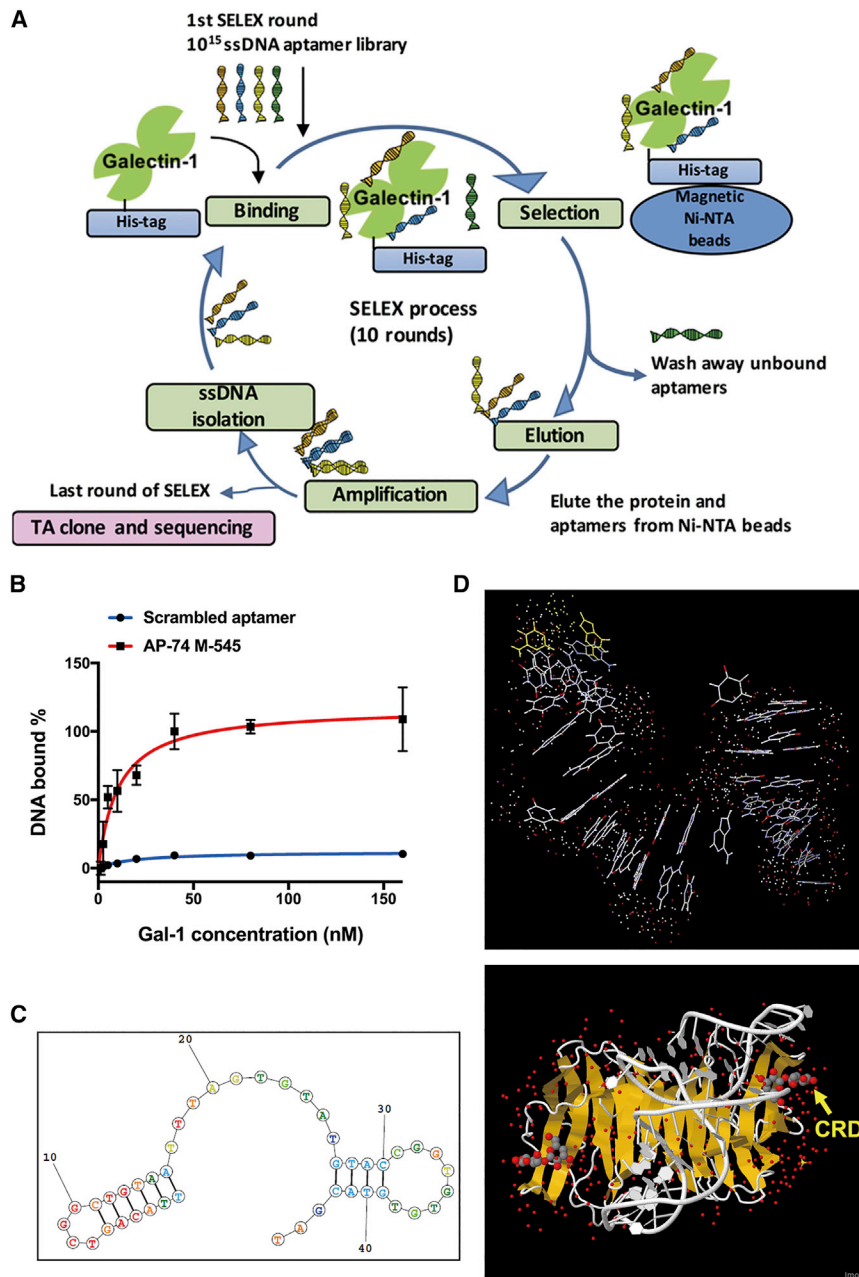
Figure 1. AP-74 M-545, a Gal-1-Targeting Aptamer, Binds to the CRD of Gal-1

(A) Schematic illustration of His-tagged recombinant Gal-1 SELEX. (B) The dissociation constant of AP-74 M-545 was analyzed by using a nitrocellulose filter binding assay (n = 3) and calculated with GraphPad software. (C) The predicted secondary structure of AP-74 M-545. (D) The predicted 3D structure of AP-74 M-545 (top) and the docking simulation of AP-74 M-545 (light gray) with Gal-1 protein (red and gray) (bottom). The yellow arrow points to the CRD of the Gal-1 protein.

Therefore, in this study, we focused on the extracellular functions of Gal-1 and selected specific DNA aptamers to target Gal-1. We used recombinant Gal-1 to screen DNA aptamers and identify a Gal-1-targeting aptamer, AP-74 M-545, after systematic evolution of ligands by exponential enrichment (SELEX) and aptamer array processes. We further used lung cancer mouse models to investigate the characteristics, functions, and effects of the Gal-1 aptamers. Our results show that AP-74 M-545 binds to human and mouse Gal-1, leading to T cell apoptosis restoration and tumor growth inhibition. These data suggest that AP-74 M-545 could be developed into a potential therapeutic strategy in cancer immunotherapy.
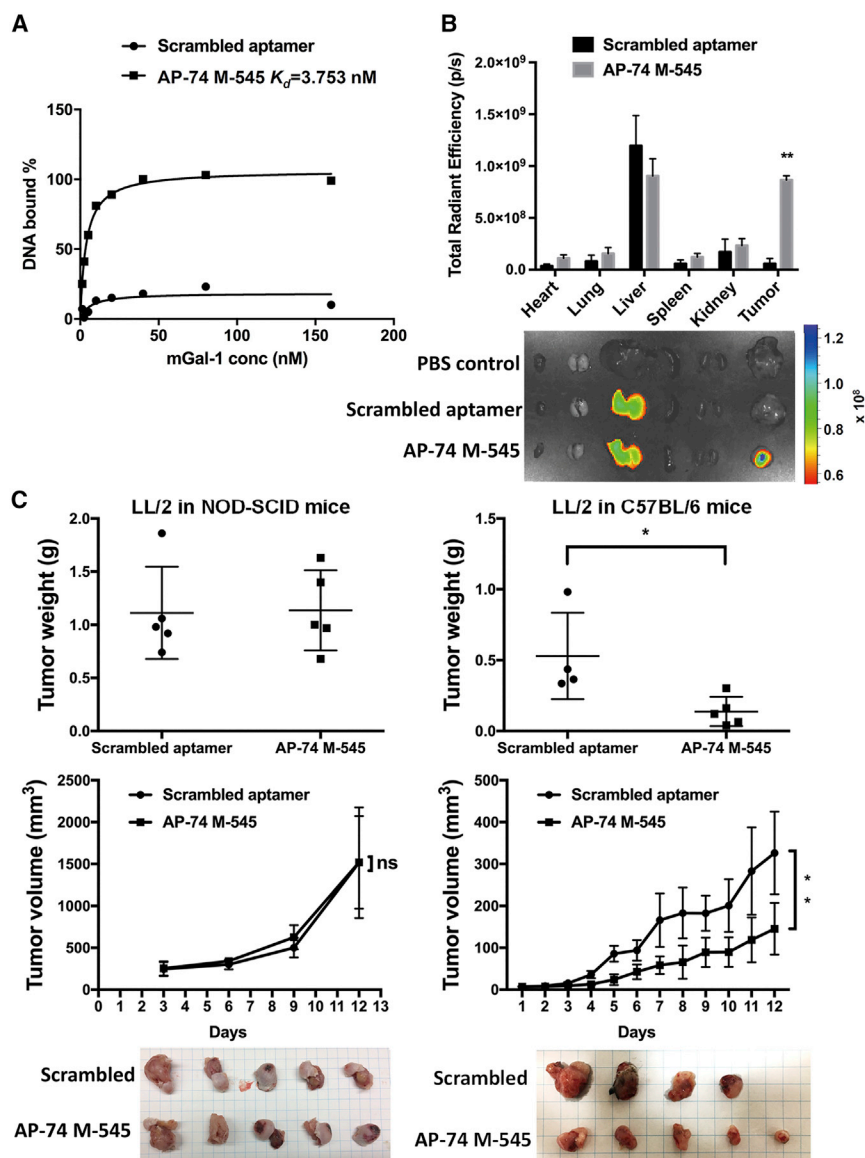
RESULTS

Gal-1-Targeting Aptamers Were Selected by His-Tagged Recombinant Protein SELEX

To identify the Gal-1-targeting aptamers, 10^{15} molecules of a random-sequence aptamer library were used to perform recombinant protein SELEX. The SELEX process was completed at the 10th round, and the selected aptamers were identified by TA cloning and DNA sequencing (Figure 1A). The aptamer candidates were analyzed by the sequence alignment software Clustal Omega[21] and FASTAptamer.[22]

To shorten the aptamers and identify the binding region of aptamers to Gal-1, we designed and shortened aptamers by making customized synthetic aptamer arrays (Figure S1). According to the results of the aptamer array, we selected six short aptamer candidates for further analysis (Table S1). The binding affinity of AP-74 M-545, which showed the highest intensity on the aptamer array, was still high and comparable to full-length AP-74. AP-74 M-545 specifically bound to recombinant human Gal-1, with a K_D of 3.747 nmol/L (Figure 1B). Therefore, we chose AP-74 M-545 as our research target. The secondary structure prediction by M-fold showed that AP-74 M-545 contains two stem-loop structures at its 3′ and 5′ ends (Figure 1C).

aptamers can also be modified by fluorescence, biotin, or nanoparticles.[17,18] Modified aptamers can label or kill tumors that express specific markers. For example, the aptamer of CD70, which is conjugated with ATTO-647N fluorescence, acts as an "aptasensor" for the sensitive and fast detection of CD70-positive SKOV-3.[19] In an immunotherapeutic study, a programmed cell death ligand-1 (PD-L1)-targeting aptamer suppressed tumor growth by increasing the number of tumor-infiltrating T cells.[20]

Because of the important roles of Gal-1 in cancer progression and immune escape, Gal-1 could be a potential immunotherapy target.

Figure 2. AP-74 M-545 Accumulates in Tumors and Suppresses Tumor Growth Only in LL/2 Lung Cancer C57BL/6 Murine Tumor Models

(A) The dissociation constant of AP-74 M-545 to murine Gal-1 was analyzed by using a nitrocellulose filter binding assay ($n = 3$) and calculated with GraphPad software. (B) Biodistribution of the IRDye 800-scrambled aptamer or IRDye 800-AP-74 M-545 (1 µg) 6 h after intraperitoneal injection ($n = 4$ mice/group). (C) The scrambled aptamer (2 mg/kg, $n = 5$) or AP-74 M-545 (2 mg/kg, $n = 5$) was injected intratumorally. The data are presented as the mean ± SEM and were analyzed by Student's t test. *$P < 0.05$, **$P < 0.01$.

IRDye 800-labeled aptamers were intraperitoneally injected into LL/2-bearing mice. The fluorescence signals of AP-74 M-545 in tumor tissues were significantly higher than those of the scrambled aptamers after 6 h of injection (Figure 2B). The intensity of the fluorescence signals of both the scrambled and AP-74 M-545 aptamers was similar in the liver, most likely because the DNA aptamers were metabolized mainly by the liver. The similar result of biodistribution was also observed in an LL/2 orthotopic lung cancer mouse model (Figure S2). The expression of Gal-1 was further examined and showed that the level of Gal-1 in tumor tissue was much higher than in other organs (Figure S3). These results suggest that AP-74 M-545 accumulates in tumor tissues by targeting Gal-1-overexpressing tumor cells and stromal cells. The tumor inhibitory function of AP-74 M-545 was further investigated in a murine syngeneic model and in immune-deficient non-obese diabetic (NOD)/severe combined immunodeficiency (SCID) mice. Intriguingly, AP-74 M-545 suppressed tumor growth only in C57BL/6 mice but not in NOD/SCID mice after intratumoral injection (Figure 2C). These data suggest that the tumor-suppressive effect of AP-74 M-545 might be associated with immune regulation.

The prediction of the 3D structure and docking site further revealed that AP-74 M-545 might block the carbohydrate recognition domain of Gal-1 (Figure 1D). These data show that AP-74 M-545 binds to recombinant Gal-1.

AP74-M-545 Targets LL/2 Tumor Tissues and Suppresses Tumor Growth

To investigate the functions of AP-74 M-545 *in vivo*, the LL/2 murine syngeneic tumor model was established. First, we examined the interaction between the aptamers and murine Gal-1. The amino acid residues of human and murine Gal-1 share 88% identity. The binding assay revealed that AP-74 M-545 bound to recombinant murine Gal-1, with a K_D of 3.753 nmol/L (Figure 2A). We further evaluated the biodistribution of AP-74 M-545 *in vivo*.

AP-74 M-545 Increases Infiltrated CD4^{+} and CD8^{+} T Cells in Tumor Tissues

Tumor-derived Gal-1 has been reported to mediate tumor immune escape by inducing T cell apoptosis. To address whether the tumor suppression of AP-74 M-545 occurred via immune regulation, we further assessed the numbers of infiltrated CD4 and CD8 T cells in AP-74 M-545- and scrambled aptamer-treated tumor tissues. The immunohistochemistry staining analysis showed that the numbers of infiltrated CD4^{+} and CD8^{+} T cells were increased in tumor tissues of the AP-74 M-545-treated group (Figure 3). This result indicates that AP-74 M-545 suppresses tumor growth by increasing the
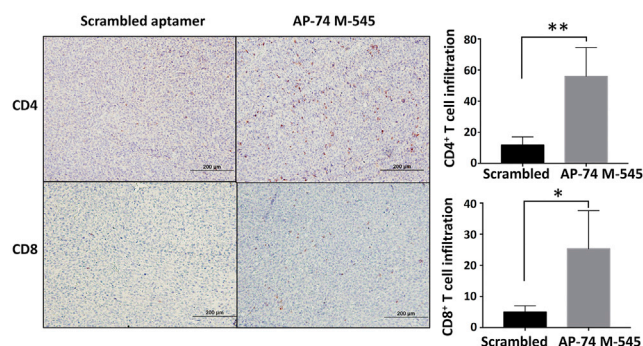
Figure 3. Tumor-Infiltrating CD4 and CD8 T Cells Are Increased in AP-74 M-545-Treated Tumors

Tumor-infiltrating CD4 and CD8 T cells were detected by immunochemistry staining. The data are presented as the mean ± SEM and were analyzed by Student's t test. *P < 0.05, **P < 0.01.

T cell infiltration. An *in vitro* cell proliferation assay was performed to further exclude the direct growth inhibition of AP-74 M-545 on LL/2 cells. After aptamer treatment, the proliferation of LL/2 cells was not repressed by AP-74 M-545 (Figure S4). The vessels in tumor tissues were also analyzed by CD31 immunohistochemistry staining. However, the number of vessels was not significantly different between the scrambled aptamer- or AP-74 M-545-treated groups (Figure S5). Thus, these results suggest that AP-74 M-545 inhibits tumor growth mainly by blocking Gal-1-mediated immune regulation.

AP-74 M-545 Blocks the Binding of Gal-1 to T Cells and Reduces Gal-1-Mediated T Cell Apoptosis

Previous reports have indicated that Gal-1 mediates T cell apoptosis by binding to T cell receptors such as CD45.[23] We next investigated whether AP-74 M-545 blocked the binding of Gal-1 to T cells. Flow cytometry analyses showed that AP-74 M-545 reduced the binding of fluorescein isothiocyanate (FITC)-Gal-1 to T cells in a dose-dependent manner (Figure 4A). This result suggested that Gal-1-mediated T cell apoptosis could be rescued by AP-74 M-545. Therefore, we further examined whether AP-74 M-545 inhibited T cell apoptosis mediated by Gal-1. To examine T cell apoptosis, annexin V and propidium iodide (PI) staining of T cells was analyzed by flow cytometry. The apoptosis analysis revealed that AP-75 M-545 inhibited Gal-1-induced T cell apoptosis (Figure 4B). These results suggest that AP-74 M-545 reduces T cell apoptosis by blocking the binding of Gal-1 to T cells.

AP-74 M-545 Blocks the Binding of Gal-1 to CD45 and Rescues IL-2 Expression

We next determined whether AP-74 M-545 could block the biological activities of Gal-1. The binding of Gal-1 to CD45 on T cells has been reported to transduce apoptotic signal.[23] Therefore, we wanted to confirm whether this binding could be blocked by AP-74 M-545. The binding of biotin-labeled Gal-1 to coated CD45 was analyzed by an ELISA. The binding was blocked by AP-74 M-545 but not by the scrambled aptamer in a dose-dependent manner (Figure 5A). Previous studies have shown that Gal-1 inhibited T cell activation and

downregulated interleukin-2 (IL-2) expression.[10,24] Thus, we further investigated whether AP-75 M-545 recovered T cell activation and increased IL-2 expression. The results of the T cell activation bioassay (IL-2) showed that AP-75 M-545 elevated the IL-2 bioluminescent signal (Figure 5B). Moreover, we further investigated the expression of IL-2 in aptamer-treated LL/2 tumors *in vivo*. The expression of IL-2 was increased in the AP-75 M-545-treated group according to immunoblot analyses (Figure 5C). These results suggest that AP-75 M-545 not only blocks the binding of Gal-1 to CD45 but also rescues IL-2 expression.

DISCUSSION

Gal-1 is a member of the galectin family that exists as a homodimeric protein with two carbohydrate recognition domains (CRDs). Previous studies support that the involvement of Gal-1 contributes to tumor progression (i.e., tumor growth, angiogenesis, metastasis, and tumor cell migration). Most importantly, increasing evidence has indicated that Gal-1 suppresses the tumor immune response due to its immunosuppressive effect. Thus, overcoming Gal-1-mediated tumor immune escape is an important issue in cancer therapy.

Here, we developed the first Gal-1-targeting DNA aptamer, AP-74 M-545, and demonstrated that it suppresses tumor growth by affecting the tumor immune response. AP-74 M-545 exhibited antitumor effects in wild-type C57BL/6 mice but not in immunodeficient NOD/SCID mice by increasing the number of tumor-infiltrated CD4^{+} and CD8^{+} T cells. Similar results were observed in Gal-1-knockdown murine breast cancer models.[25] Increased CD4^{+} and CD8^{+} T cells in tumor tissues were also observed in mice treated with Gal-1-targeted short hairpin RNA (shRNA). These results suggest that targeting Gal-1 could be a feasible and novel strategy to restore tumor-specific immune cells. To explore the underlying mechanisms, we demonstrated that AP-74 M-545 blocked the binding of Gal-1 to CD45, the major Gal-1 binding receptor on T cells, and reduced Gal-1-mediated T cell apoptosis *in vitro*. In addition to reducing T cells apoptosis, AP-74 M-545 also increased the expression of IL-2, an important factor for the activation of the immune system,[26] indicating that targeting Gal-1 by aptamers not only rescues but also activates immune function. Our research is the first to use an aptamer to target Gal-1 and examine its cancer immune escape function and provide a useful way to eradicate cancer.

To date, several Gal-1 inhibitors have been developed and studied in cancer therapeutic research such as thiodigalactoside (TDG),[27] OTX008,[28] anginex (β pep-25),[29] and GM-CT-01.[30] These inhibitors contribute to tumor growth inhibition and antiangiogenesis and reduce the dissemination of tumor cells.[31] Among these inhibitors, TDG and GM-CT-01 are similar to AP-74 M-545 and restored T cell surveillance in a murine model.[27,32] However, AP-74 M-545 also rescued the expression of IL-2, indicating that AP-74 M-545 acts as a Gal-1 inhibitor and simultaneously increases and activates T cells. However, unlike other Gal-1 inhibitors, AP-74 M-545 did not inhibit tumor cell growth directly *in vivo* or *in vitro*. Although cell growth is not repressed by AP-74 M-545, AP-74 M-545 does

A

B
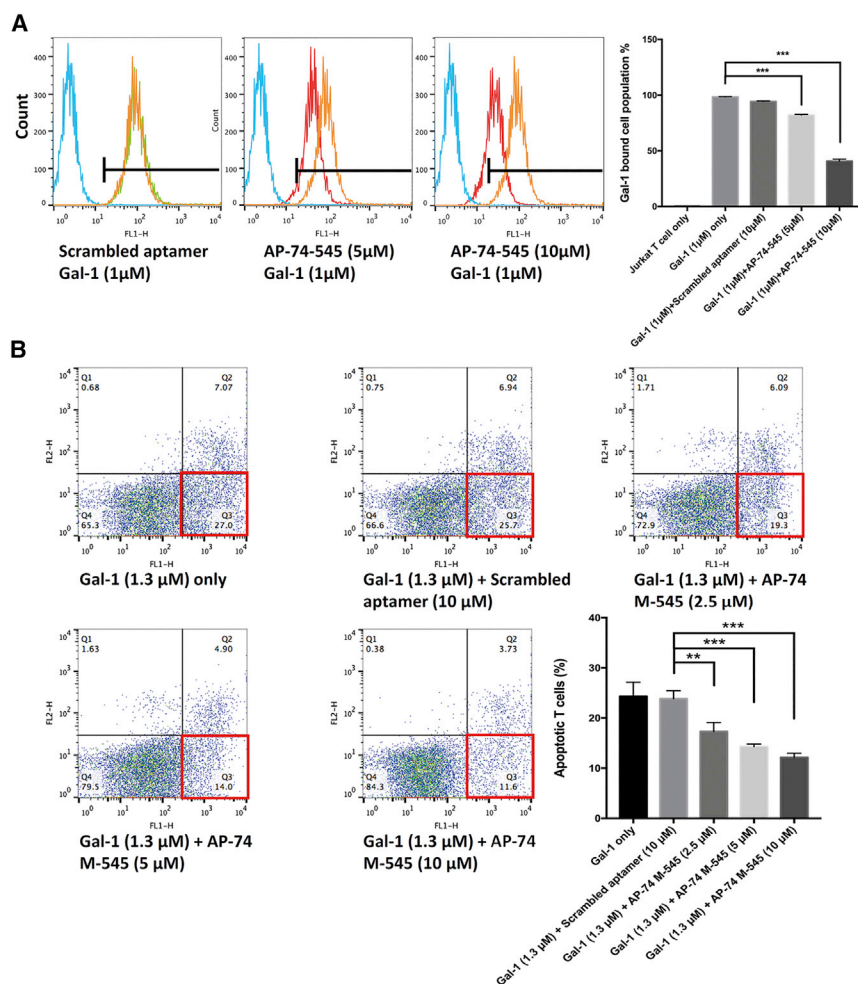
Figure 4. AP-74 M-545 Blocks the Binding of Gal-1 to T Cells and Reduces the Gal-1-Mediated T Cell Apoptosis

(A) AP-74 M-545 dose-dependently blocked the binding of FITC-Gal-1 (1 μM) to Jurkat T cells. Blue peak, T cell only; orange peak, Gal-1 FITC only; green peak, Gal-1 FITC + scrambled aptamer; red peak, Gal-1 FITC + AP-74 M-545. (B) AP-74 M-545 dose-dependently reduced Gal-1 (1.3 μM)-induced T cell apoptosis by annexin V (FL-1)-PI (FL-2) staining. The data are presented as the mean ± SEM and were analyzed by Student's t test. **$P < 0.01$, ***$P < 0.001$.

Aptamers are natural oligonucleotides and are selected for therapeutic applications with many advantages, such as low immunogenicity, low chemical toxicity, and ease of metabolizing. However, the rates of degradation and metabolism are major concerns of aptamer-based therapeutics for clinical applications. Previous studies have revealed that the half-life of unmodified aptamers is only 4–6 h *in vivo*.[34] In view of its short half-life, the further approach to extend the residence time of an aptamer is an important issue. The current research focused on improving three aspects: nuclease resistance, increasing the binding affinity or target selectivity, and the resistance of renal clearance.[35] In our study, AP-74 M-545 targeted the tumor tissue in a murine model, with a 0.97 ± 0.14 tumor-to-liver ratio, and could even be rapidly metabolized by the liver. However, Gal-1 aptamers must be modified to extend the retention time *in vivo* for further clinical use.

not affect the functions of normal cells. We demonstrated the possibility of testing the effects of aptamers on normal lung bronchus cells. Although some Gal-1 inhibitors have been found to inhibit tumor angiogenesis, we found that the number of blood vessels was not significantly changed in AP-74 M-545-treated tumors. These data suggest that without the immune system, AP-74 M-545 does not inhibit tumor growth by affecting tumor cell growth or angiogenesis, and this finding was proven in immune-deficient mice. Previous studies have revealed that Gal-1 also promotes tumor metastasis. Some Gal-1 inhibitors have been demonstrated to reduce cancer cell migration and metastasis. For example, TDG reduces murine lung metastasis by inhibiting Gal-1-mediated cancer cell adhesion to the basement membrane and endothelial cell surfaces.[33] These findings suggest that targeting Gal-1 may represent a promising and effective antimetastatic therapy. Although our study did not focus on cancer metastasis, we tested whether AP-74 M-545 affects cancer cell migration. We found that AP-74 M-545 suppressed the migration of lung cancer cells *in vitro* (data not shown). However, the antimetastatic effect of AP-74 M-545 requires additional experimental evidence in the future.

Therefore, modifying the Gal-1 aptamer to prolong its half-life will be our next goal.
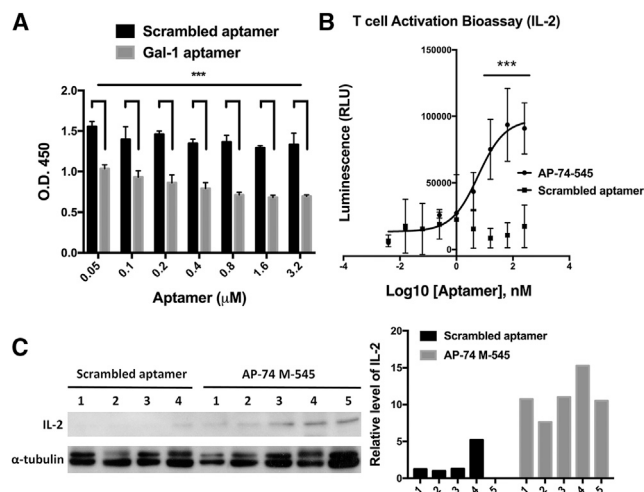
In summary, we developed a Gal-1-targeting aptamer, AP-74 M-545, that inhibits tumor growth by reducing T cell apoptosis. We demonstrated that AP-74 M-545 blocked the binding of Gal-1 to T cells and its receptor, CD45. These findings provide a novel targeting strategy for Gal-1 in cancer immune escape.

MATERIALS AND METHODS

Aptamers

All ssDNA aptamers were synthesized by Integrated DNA Technologies (IDT, Coralville, IA, USA). The ssDNA library used in the SELEX process was composed of 40-nt-long random sequences flanked by the amplifying primer sequences, 5′-ACG CTCGGATGCCACTACAG-[N]$_{40}$-CTCATGGACGTGCTGGTG AC-3′ (N = A, T, C, or G). The sequences of primers used for amplifying aptamers were forward, 5′-ACGCTCGGATGCCAC TACAG-3′ and biotin-labeled reverse, 5′-GTCACCAGCACGTCCA TGAG-3′.

Figure 5. AP-74 M-545 Blocks the Binding of Gal-1 to CD45 and Rescues IL-2 Expression

(A) Ap-74 M-545 decreased the binding of Gal-1 to CD45. (B) T cell activation was detected by a T cell activation bioassay. (C) The expression level of IL-2 was increased in AP-74 M-545-treated tumor tissues from a murine model. The CD45 binding assay results are presented as the mean ± SEM and were analyzed by Student's t test. ***$P < 0.001$.

Cell Culture

The human lung cancer cell line CL1-5 was cultured in RPMI 1640 medium (Gibco, Life Technologies, USA). The murine lung cancer cell line LL/2 was cultured in DMEM (Gibco). The Jurkat T cell line was cultured in RPMI 1640 medium (Gibco). All culture media were supplemented with 10% fetal bovine serum (Gibco).

Recombinant His-Tag Protein SELEX

The human Gal-1-targeting aptamer was isolated by using a His-tag protein SELEX method. Recombinant his-tagged human full-length Gal-1 protein was expressed by *E. coli* and confirmed to be a dimer form by mass spectrometry. In the first round of SELEX, the ssDNA library containing 10^{15} molecules was incubated with 2 μg of recombinant his-tagged human full-length Gal-1 protein and nickel-nitrilotriacetic acid (Ni-NTA) magnetic agarose beads at 25°C for 30 min in His-tag binding buffer (2.95 mM KCl, 1 mM $MgCl_2$, 2.4 mM $CaCl_2$, 0.1% Tween 20, and 10 mM imidazole in 1× PBS, pH 7.0). Ni-NTA magnetic agarose beads that bound with Gal-1 and aptamers were precipitated using a magnet. The unbound aptamers were washed out by repetitive washing with binding buffer. The Gal-1 was eluted together with Gal-1-bound aptamers by His-tag elution buffer (500 mM imidazole and 0.02% Tween 20 in PBS). After the 10th round of SELEX, Gal-1 bound aptamers were cloned to TA vectors and sequenced.

Customized Synthetic Aptamer Microarray

The sequences of Gal-1-binding aptamers were shortened and designed by using software from Academia Sinica, Taiwan. All of the sequences were then synthesized by CustomArray (WA, USA)

in duplicate to decrease oligonucleotide dropout and increase uniformity.

Nitrocellulose Filter Binding Assay

Biotin-labeled candidate aptamers were incubated with serially diluted recombinant human Gal-1 protein (1.25, 2.5, 5, 10, 20, 40, 80, and 160 nM) or mouse Gal-1 protein (1.25, 2.5, 5, 10, 20, 40, 80, and 160 nM) at 37°C for 30 min in SELEX buffer. The aptamer-bound Gal-1 protein was collected on a nitrocellulose filter, and the nitrocellulose filter was blocked with 5% BSA for 30 min at room temperature (RT). The nitrocellulose filter was incubated with horseradish peroxidase (HRP)-conjugated streptavidin for 30 min at RT and washed three times with SELEX buffer. The nitrocellulose filter was incubated with Luminata Crescendo Western HRP substrate (Millipore, MA, USA) for 1 min and exposed to X-ray film. The quantification of each bound aptamer spot was determined by ImageJ software, and the K_D of the aptamer for human or mouse Gal-1 recombinant protein was calculated with GraphPad Prism 5 software (GraphPad, San Diego, CA, USA) using the equation, $Y = A_{max} \times X/(K_D + X)$.

Aptamer Structure and Aptamer/Protein Docking Site Prediction

The secondary structure of AP-74 M-545 was predicted by M-fold web software (http://unafold.rna.albany.edu/?q=mfold/DNA-Folding-Form). Because of the lack of ssDNA 3D structure prediction software, the 3D structure of AP-74 M-545 was predicted by modeling as an RNA aptamer using RNAComposer (http://rnacomposer.cs.put.poznan.pl/). The docking sites of the AP-74 M-545 and Gal-1 (PDB: 1GZW) proteins were predicted by using the PatchDock server (http://bioinfo3d.cs.tau.ac.il/PatchDock/).

Mouse Syngeneic Tumor Model

LL/2 cells (1×10^5) were injected subcutaneously into C57BL/6 mice. Mice were randomly separated into two groups, those that received scrambled random oligonucleotides (2 mg/kg) or AP-74 M-545 (2 mg/kg), until the long axis of the tumors reached 2–3 mm. Scrambled random oligonucleotides (n = 5 mice/group) or AP-74 M-545 (n = 5 mice/group) was administered once by intratumoral injection when the tumors reached 2–3 mm. The body weight of each mouse was measured before and after aptamer treatment. All animal experiments were performed according to guidelines of the Animal Care Ethics Commission using a standard protocol approved by the Laboratory Animal Center, College of Medicine, National Cheng Kung University, Tainan, Taiwan.

Biodistribution of AP-74 M-545

The 5′ IRDye 800-labeled scrambled aptamer (1 μg) or AP-74 M-545 (1 μg) was injected intraperitoneally into two groups of LL/2 tumor-bearing mice. The mice were sacrificed 6 h after injection. Tumors and other organs (hearts, livers, spleens, lungs, and kidneys) were collected and the fluorescent signals of these tissues were emitted and detected by a Xenogen IVIS (*in vivo* imaging system) Spectrum noninvasive quantitative molecular imaging system (Caliper Life Sciences, PerkinElmer). The average fluorescent signal from the PBS-treated group was defined as the background signal in the analysis and statistics.

Binding of Gal-1 to CD45 by ELISA

Recombinant human CD45 (1430-CD, R&D Systems) was coated onto a 96-well plate (25 ng/well) at 4°C overnight. After coating, the coated wells were blocked with 1% BSA in PBS for 1 h at RT. Biotin-labeled Gal-1 (0.5 μg/mL), which was preincubated with scrambled aptamer or AP-74 M-545 (3.2 to 0.050 μM, 2-fold serial dilution) for 1 h, was added to each CD45-coated well and incubated for 1 h at RT. The plates were washed with PBS and incubated with streptavidin-HRP diluted in PBS containing 1% BSA for 1 h at RT. The plates were washed with PBS. 3,3′,5,5′-Tetramethylbenzidine (TMB) substrate (Thermo Scientific) was added and incubated for 15 min. The reaction was stopped with 2 N H_2SO_4. The absorbance at optical density 450 (OD_{450}) was read by a microplate ELISA reader (Tecan).

Immunohistochemical Staining of Tumor

Scrambled aptamer- and AP-74 M-545-treated tumor tissues were collected, fixed in 10% formalin, dehydrated, and embedded in paraffin. 5-μm-thick tissue sections were sliced, deparaffinized, rehydrated, and heated for 40 min for antigen retrieval in citrate buffer (pH 6.0). Primary antibodies against mouse CD4 (Thermo Scientific), CD8 (Thermo Scientific), or CD31 (Abcam) were diluted in antibody diluent (Biocare Medical) at a 1:200 dilution. Biotin-labeled anti-rat and anti-rabbit secondary antibodies (Jackson Laboratory) were used in a 1:200 dilution. Streptavidin-HRP were used to detect the antigens and visualized by 3-amino-9-ethylcarbazole (AEC) substrate-chromogen (Dako), followed by hematoxylin counterstain.

Flow Cytometry Analysis

FITC-labeled Gal-1 (1 μM) or FITC-labeled Gal-1 that was preincubated with scrambled or AP-74 M-545 aptamer (5 and 10 μM) was added to Jurkat T cells for 60 min at 4°C. These FITC signals of Gal-1-treated Jurkat T cells were further washed and analyzed by a FACSCalibur cell analyzer (BD). In the T cell apoptosis assay, Gal-1 (1.3 μM), which was preincubated with scrambled or AP-74 M-545 (2.5, 5, and 10 μM) aptamer, was added to 1×10^5 Jurkat T cells for 12 h at 37°C. The Gal-1-treated Jurkat T cells were collected and stained by an FITC annexin V/PI kit (Invitrogen). The staining T cells were washed and analyzed by a FACSCalibur cell analyzer (BD).

T Cell Activation Bioassay (IL-2)

The Gal-1 highly expressed CL1-5 cells were seeded at 4×10^4/well in 96-well plates. Scrambled or AP-74 M-545 aptamers were prepared in 4-fold serial dilution (from 256 to 0.0039 nM) and added to the pre-plated CL1-5 cells. TCR/CD3 effector cells (IL-2) at 1×10^5/well were added to each well containing CL1-5 and aptamer dilutions at 37°C for 6 h. 75 μL of Bio-Glo reagent was added to each well of the assay plate and incubated at 37°C for 10 min. Luminescence was detected by using a luminescence plate reader.

Western Blotting

Total proteins were extracted from aptamer-treated tumors in murine model using a radioimmunoprecipitation assay (RIPA) buffer con-taining protease inhibitor cocktail (Roche Applied Science). Primary antibodies against the murine IL-2 (Abcam) and α-tubulin (Sigma) were used at a 1:5,000 dilution. HRP-labeled secondary antibodies were used at a 1:5,000 dilution (Santa Cruz Biotechnology).

Statistical Analysis

The data in bar graphs were presented as means ± standard error of the mean and were analyzed using a Student's t test. A p value < 0.05 was considered statistically significant.

SUPPLEMENTAL INFORMATION

Supplemental Information can be found online at https://doi.org/10.1016/j.omtn.2019.10.029.

AUTHOR CONTRIBUTIONS

CONFLICTS OF INTEREST

The authors declare no competing interests.

ACKNOWLEDGMENTS

REFERENCES

1. Eggermont, A.M., Chiarion-Sileni, V., Grob, J.J., Dummer, R., Wolchok, J.D., Schmidt, H., Hamid, O., Robert, C., Ascierto, P.A., Richards, J.M., et al. (2016). Prolonged survival in stage III melanoma with ipilimumab adjuvant therapy. N. Engl. J. Med. 375, 1845–1855.

2. Hamid, O., Robert, C., Daud, A., Hodi, F.S., Hwu, W.J., Kefford, R., Wolchok, J.D., Hersey, P., Joseph, R.W., Weber, J.S., et al. (2013). Safety and tumor responses with lambrolizumab (anti-PD-1) in melanoma. N. Engl. J. Med. 369, 134–144.

3. Beatty, G.L., and Gladney, W.L. (2015). Immune escape mechanisms as a guide for cancer immunotherapy. Clin. Cancer Res. 21, 687–692.

4. Taube, J.M., Anders, R.A., Young, G.D., Xu, H., Sharma, R., McMiller, T.L., Chen, S., Klein, A.P., Pardoll, D.M., Topalian, S.L., and Chen, L. (2012). Colocalization of inflammatory response with B7-h1 expression in human melanocytic lesions supports an adaptive resistance mechanism of immune escape. Sci. Transl. Med. 4, 127ra37.

5. Earl, L.A., Bi, S., and Baum, L.G. (2011). Galectin multimerization and lattice formation are regulated by linker region structure. Glycobiology 21, 6–12.

6. Astorgues-Xerri, L., Riveiro, M.E., Tijeras-Raballand, A., Serova, M., Neuzillet, C., Albert, S., Raymond, E., and Faivre, S. (2014). Unraveling galectin-1 as a novel therapeutic target for cancer. Cancer Treat. Rev. 40, 307–319.

7. Wu, M.H., Hong, H.C., Hong, T.M., Chiang, W.F., Jin, Y.T., and Chen, Y.L. (2011). Targeting galectin-1 in carcinoma-associated fibroblasts inhibits oral squamous cell carcinoma metastasis by downregulating MCP-1/CCL2 expression. Clin. Cancer Res. 17, 1306–1316.

8. Chiang, W.F., Liu, S.Y., Fang, L.Y., Lin, C.N., Wu, M.H., Chen, Y.C., Chen, Y.L., and Jin, Y.T. (2008). Overexpression of galectin-1 at the tumor invasion front is associated with poor prognosis in early-stage oral squamous cell carcinoma. Oral Oncol. 44, 325–334.

9. Pace, K.E., Lee, C., Stewart, P.L., and Baum, L.G. (1999). Restricted receptor segregation into membrane microdomains occurs on human T cells during apoptosis induced by galectin-1. J. Immunol. 163, 3801–3811.

10. Chung, C.D., Patel, V.P., Moran, M., Lewis, L.A., and Miceli, M.C. (2000). Galectin-1 induces partial TCR ζ-chain phosphorylation and antagonizes processive TCR signal transduction. J. Immunol. 165, 3722–3729.

11. Le, Q.T., Shi, G., Cao, H., Nelson, D.W., Wang, Y., Chen, E.Y., Zhao, S., Kong, C., Richardson, D., O'Byrne, K.J., et al. (2005). Galectin-1: a link between tumor hypoxia and tumor immune privilege. J. Clin. Oncol. 23, 8932–8941.

12. Rubinstein, N., Alvarez, M., Zwirner, N.W., Toscano, M.A., Ilarregui, J.M., Bravo, A., Mordoh, J., Fainboim, L., Podhajcer, O.L., and Rabinovich, G.A. (2004). Targeted inhibition of galectin-1 gene expression in tumor cells results in heightened T cell-mediated rejection; a potential mechanism of tumor-immune privilege. Cancer Cell 5, 241–251.

13. Hsu, Y.L., Hung, J.Y., Chiang, S.Y., Jian, S.F., Wu, C.Y., Lin, Y.S., Tsai, Y.M., Chou, S.H., Tsai, M.J., and Kuo, P.L. (2016). Lung cancer-derived galectin-1 contributes to cancer associated fibroblast-mediated cancer progression and immune suppression through TDO2/kynurenine axis. Oncotarget 7, 27584–27598.

14. Tang, D., Yuan, Z., Xue, X., Lu, Z., Zhang, Y., Wang, H., Chen, M., An, Y., Wei, J., Zhu, Y., et al. (2012). High expression of Galectin-1 in pancreatic stellate cells plays a role in the development and maintenance of an immunosuppressive microenvironment in pancreatic cancer. Int. J. Cancer 130, 2337–2348.

15. Lee, J.H., Canny, M.D., De Erkenez, A., Krilleke, D., Ng, Y.S., Shima, D.T., Pardi, A., and Jucker, F. (2005). A therapeutic aptamer inhibits angiogenesis by specifically targeting the heparin binding domain of VEGF165. Proc. Natl. Acad. Sci. USA 102, 18902–18907.

16. Chang, Y.C., Kao, W.C., Wang, W.Y., Wang, W.Y., Yang, R.B., and Peck, K. (2009). Identification and characterization of oligonucleotides that inhibit Toll-like receptor 2-associated immune responses. FASEB J. 23, 3078–3088.

17. Arvand, M., and Mirroshandel, A.A. (2019). An efficient fluorescence resonance energy transfer system from quantum dots to graphene oxide nano sheets: application in a photoluminescence aptasensing probe for the sensitive detection of diazinon. Food Chem. 280, 115–122.

18. Hanif, A., Farooq, R., Rehman, M.U., Khan, R., Majid, S., and Ganaie, M.A. (2019). Aptamer based nanobiosensors: promising healthcare devices. Saudi Pharm. J. 27, 312–319.

19. Bayat, P., Taghdisi, S.M., Rafatpanah, H., Abnous, K., and Ramezani, M. (2019). In vitro selection of CD70 binding aptamer and its application in a biosensor design for sensitive detection of SKOV-3 ovarian cells. Talanta 194, 399–405.

20. Lai, W.Y., Huang, B.T., Wang, J.W., Lin, P.Y., and Yang, P.C. (2016). A novel PD-L1-targeting antagonistic DNA aptamer with antitumor effects. Mol. Ther. Nucleic Acids 5, e397.

21. Madeira, F., Park, Y.M., Lee, J., Buso, N., Gur, T., Madhusoodanan, N., Basutkar, P., Tivey, A.R.N., Potter, S.C., Finn, R.D., and Lopez, R. (2019). The EMBL-EBI search and sequence analysis tools APIs in 2019. Nucleic Acids Res. 47 (W1), W636–W641.

22. Alam, K.K., Chang, J.L., and Burke, D.H. (2015). FASTAptamer: a bioinformatic toolkit for high-throughput sequence analysis of combinatorial selections. Mol. Ther. Nucleic Acids 4, e230.

23. Perillo, N.L., Pace, K.E., Seilhamer, J.J., and Baum, L.G. (1995). Apoptosis of T cells mediated by galectin-1. Nature 378, 736–739.

24. Vespa, G.N., Lewis, L.A., Kozak, K.R., Moran, M., Nguyen, J.T., Baum, L.G., and Miceli, M.C. (1999). Galectin-1 specifically modulates TCR signals to enhance TCR apoptosis but inhibit IL-2 production and proliferation. J. Immunol. 162, 799–806.

25. Dalotto-Moreno, T., Croci, D.O., Cerliani, J.P., Martinez-Allo, V.C., Dergan-Dylon, S., Méndez-Huergo, S.P., Stupirski, J.C., Mazal, D., Osinaga, E., Toscano, M.A., et al. (2013). Targeting galectin-1 overcomes breast cancer-associated immunosuppression and prevents metastatic disease. Cancer Res. 73, 1107–1117.

26. Jiang, T., Zhou, C., and Ren, S. (2016). Role of IL-2 in cancer immunotherapy. OncoImmunology 5, e1163462.

27. Ito, K., Scott, S.A., Cutler, S., Dong, L.F., Neuzil, J., Blanchard, H., and Ralph, S.J. (2011). Thiodigalactoside inhibits murine cancers by concurrently blocking effects of galectin-1 on immune dysregulation, angiogenesis and protection against oxidative stress. Angiogenesis 14, 293–307.

28. Dings, R.P., Miller, M.C., Nesmelova, I., Astorgues-Xerri, L., Kumar, N., Serova, M., Chen, X., Raymond, E., Hoye, T.R., and Mayo, K.H. (2012). Antitumor agent calixarene 0118 targets human galectin-1 as an allosteric inhibitor of carbohydrate binding. J. Med. Chem. 55, 5121–5129.

29. Dong, D.F., Li, E.X., Wang, J.B., Wu, Y.Y., Shi, F., Guo, J.J., Wu, Y., Liu, J.P., Liu, S.X., and Yang, G.X. (2009). Anti-angiogenesis and anti-tumor effects of AdNT4-anginex. Cancer Lett. 285, 218–224.

30. Miller, M.C., Klyosov, A., and Mayo, K.H. (2009). The α-galactomannan Davanat binds galectin-1 at a site different from the conventional galectin carbohydrate binding domain. Glycobiology 19, 1034–1045.

31. Wdowiak, K., Francuz, T., Gallego-Colon, E., Ruiz-Agamez, N., Kubeczko, M., Grochoła, I., and Wojnar, J. (2018). Galectin targeted therapy in oncology: current knowledge and perspectives. Int. J. Mol. Sci. 19, E210.

32. Demotte, N., Bigirimana, R., Wieërs, G., Stroobant, V., Squifflet, J.L., Carrasco, J., Thielemans, K., Baurain, J.F., Van Der Smissen, P., Courtoy, P.J., and van der Bruggen, P. (2014). A short treatment with galactomannan GM-CT-01 corrects the functions of freshly isolated human tumor-infiltrating lymphocytes. Clin. Cancer Res. 20, 1823–1833.

33. Ito, K., and Ralph, S.J. (2012). Inhibiting galectin-1 reduces murine lung metastasis with increased CD4+ and CD8+ T cells and reduced cancer cell adherence. Clin. Exp. Metastasis 29, 561–572.

34. Keefe, A.D., Pai, S., and Ellington, A. (2010). Aptamers as therapeutics. Nat. Rev. Drug Discov. 9, 537–550.

35. Ni, S., Yao, H., Wang, L., Lu, J., Jiang, F., Lu, A., and Zhang, G. (2017). Chemical modifications of nucleic acid aptamers for therapeutic purposes. Int. J. Mol. Sci. 18, E1683.